In-situ end-point detection during ion-beam etching of multilayer dielectric gratings

Hua Lin (林 华), Lifeng Li (李立峰), and Lijiang Zeng (曾理江)

State Key Laboratory of Precision Measurement Technology and Instruments, Department of Precision Instruments, Tsinghua University, Beijing 100084

Received July 21, 2004

An *in-situ* end-point detection technique for ion-beam etching is presented. A laser beam of the same wavelength and polarization as those in the intended application of the grating is fed into the vacuum chamber, and the beam retro-diffracted by the grating under etching is extracted and detected outside the chamber. This arrangement greatly simplifies the end-point detection. Modeling the grating diffraction with a rigorous diffraction grating computer program, we can satisfactorily simulate the evolution of the diffraction intensity during the etching process and consequently, we can accurately predict the end-point. Employing the proposed technique, we have reproducibly fabricated multilayer dielectric gratings with diffraction efficiencies of more than 92%.

OCIS codes: 050.0050, 050.1950, 050.2770.

Diffraction gratings used in high-power laser systems are required to possess high diffraction efficiency and high laser damage threshold. Multilayer dielectric gratings consisting of a transmission surface-relief grating atop a highly reflecting dielectric thin-film stack can meet these two requirements[1,2]. To create the top surface corrugation, a photoresist grating mask is first made by holographic means on the thin-film stack, followed by ion-beam etching (IBE) into the top dielectric layer. Given the fact that the diffraction efficiency of a multilayer dielectric grating greatly depends on its groove depth, accurate end-point control becomes a critical issue in the etching process. One established approach is to measure the etched depth of a sacrificial sample by scanning electron microscope (SEM). Unfortunately, SEM approach is destructive, time-consuming, expensive, and off-line. An alternative method is to take the grating out off the chamber, remove a small area of the photoresist and measure the efficiency from time to time during etching. Though this approach achieves better cost-efficiency than the SEM approach, it is clearly undesirable since it is an *ex-situ* approach and is very inefficient. The importance of *in-situ* end-point detection has been highly recognized in the field of microelectronics fabrication and many detection approaches have been proposed[3−5]. But these methods either entail expensive instruments or require the sample's bar and groove to be larger than light spot or an etch stop layer as end-point, which make them not straightforwardly applicable to the fabrication of multilayer dielectric gratings. Svakhin *et al.*[6] presented a feasible method by monitoring grating diffraction, but their monitoring, strictly speaking, is not an *in-situ* one. In addition, because the decision was based on the relative diffraction efficiency, the reflected intensity needed to be measured.

In this letter, we propose an *in-situ* end-point detection scheme for fabricating multilayer dielectric gratings. According to our design, the gratings are potentially capable of placing up to 99% of the incident light into a single diffraction order and could achieve high diffraction efficiency within a wide range of groove depths ($0.18 - 0.30$ μm) and duty cycles ($0.25 - 0.5$). To get the desired groove profile parameters, an *in-situ* monitoring system is set up as follows. During etching, a laser beam of the same wavelength and polarization as those in the intended application of the grating is fed into the vacuum chamber, and the beam retro-diffracted by the grating under etching is extracted and detected outside the chamber. In this way, the problem of end-point detection is greatly simplified and as shown in the following discussion, the etching procedure can be insured to stop at an optimal point to prevent excessive etching. More importantly, the repeatability of fabricating high efficiency gratings can be guaranteed with the proposed framework. It should be noticed that, compared with the off-line methods, a big advantage of the proposed approach is that there is no need to stop etching and measure the diffraction efficiency from time to time by taking the grating out of the vacuum chamber.

The grating quality relies on the fabrication process significantly. In our work, photoresist grating masks meeting the requirements for etching are first fabricated. *In-situ* monitoring systems[7,8] are used to control the profile by terminating the exposure and development steps at the optimal moments. Typical profiles of our photoresist grating masks are rectangular with vertical wall of $0.75-0.85$ μm high, clean troughs, and a duty cycle of 0.3. We measure the grating efficiency before etching, and refer it as an estimation of the groove depth of the mask. Then, the periodic pattern is transferred into the top hafnia layer by ion-beam etching with Ar^+ as the working gas. Since time-based control is ineffective, and it is necessary to terminate the IBE at the optimal moment to obtain a desired depth, we choose to monitor the intensity of the -1st-order retro-diffraction intensity during IBE. The *in-situ* end-point detection system and the etching apparatus are illustrated in Fig. 1. A photoresist grating mask is placed on a rotatable sample holder. The grating plane is oriented perpendicular to the rotation axis. A laser beam with a wavelength of 1.064 μm and transverse

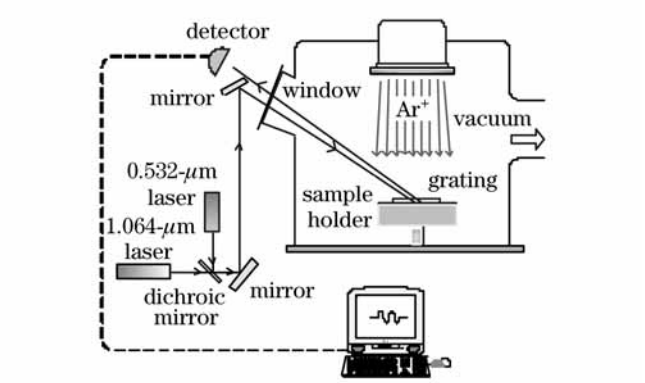

Fig. 1. The *in-situ* end-point detection system and ion-beam etching apparatus.

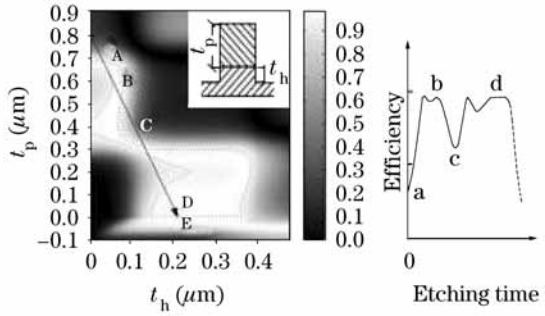

Fig. 2. Combined effect of photoresist and hafnia groove depths on the diffraction efficiency (duty cycle = 0.4). See text for more details.

electric (TE) polarization illuminates the grating via mirrors and an observation window of the vacuum chamber. The direction and position of the input laser beam and the orientation of the grating are carefully adjusted to allow the −1st-order retro-diffraction (−1st-order Littrow angle is 52°) to be detected outside of the chamber, and the time-dependent diffraction intensity is recorded by a computer. On the computer screen, we can monitor the diffraction intensity in real time. Because the laser beam is invisible, another laser with a wavelength of 0.532 μm is aligned coaxial with the infrared beam. Its −2nd-order Littrow angle is equal to the −1st-order Littrow angle of the 1.064 μm beam, which eases the work of optical adjustment. Since we need not measure the diffraction efficiency, the accurate determination of input and output intensities is not needed. This setup is simple and all the components used are outside of the vacuum which avoid being bombarded by the ion beam. And if necessary, the diffraction intensity of the green laser can be extracted for further analysis by simply placing a dichroic mirror before the detector to reflect it and detecting it by another detector.

During etching, the photoresist and the dielectric material to be removed are simultaneously etched (with different rates) under (Ar^+) ion bombardment, which makes the evolution of grating profile and composition be a complex process. In order to quantitatively characterize the combined effect of the groove depth t_h etched into the top hafnia layer and the thickness t_p of the photoresist mask, we utilize a rigorous diffraction grating computer program, Kappa (a grating simulation software written by one of the authors, L. F. Li), to calculate the diffraction efficiencies of different combinations of t_h and t_p. Because the grating is designed to have only one nonzero diffraction order, the groove shape has a negligible effect on the efficiency of the resulted grating, and to simplify the problem we assume the profile shape is rectangular. The left subfigure in Fig. 2 depicts the typical combined effect of t_h and t_p on diffraction efficiency. In particular, in region $t_p < 0$, $|t_p|$ represents the thickness removed from the top of the hafnia grating ridge after photoresist mask has been completely etched away. For any point on the figure, the sum of its coordinates ($t_p + t_h$) gives the total grating groove depth, and its gray scale depicts the associated diffraction efficiency level. The five regions A through E denote the five different stages of etching. Region A denotes the beginning of etching, where t_h is zero and only the photoresist contributes to diffraction efficiency. As the etching moves into region B, where t_p is between 0.4 and 0.65 μm and t_h is small, the efficiency reaches relatively high values. As the etching approaches region C, the efficiency decreases dramatically as expected since t_p decreases. With the increase of t_h and the decrease of t_p, the former plays a more and more important role, and subsequently, the efficiency increases until it reaches the design region D. Any point in D is a desirable end-point where we can obtain high quality gratings. Continued etching will result in over-etching (region E) which is obviously undesirable.

From the above analysis, it can be seen that although the evolution of grating profile and composition is a complex process, it leaves a clear trace when diffraction intensity is plotted against etching time. In Fig. 2, the vector from (0, 0.8) to (0.2, 0) denotes the assumed etching trail and its slope is −0.25, which implies that the original photoresist thickness is 0.8 μm and the etching ratio of photoresist over hafnia is about 4. In the right part of Fig. 2, the curve of efficiency versus etching time is plotted, where the lower case letters denote the extreme points of regions A to D. When the etching evolves into the neighborhood of point d, it should be stopped. Otherwise the intensity will abruptly decrease (shown as the dashed line which corresponds to etching into region E) and finally become zero.

Figure 3 shows the monitoring curves recorded for two different samples and the SEM pictures of the resulted gratings placed at the right side of their curves respectively. Since sputtered material polluted the observation window, the detected diffraction intensity was attenuated. Therefore the exact diffraction intensity value was not obtained, but the trend lines were correct. From the curves, we can see that at the beginning of etching, diffraction intensity reaches and keeps at high values for a while. It then starts to decrease and after a minimum point is reached, it rises gradually to a new peak. When the etching evolves into a prescribed neighborhood of the peak, it should be stopped. It is clearly seen from Fig. 3 that the main features of the monitoring curves as described above agree well with our earlier analysis. The SEM pictures of the gratings show that the gratings' groove depths and duty cycles meet our expectation quite well and their efficiencies are more than 92%.

We notice that in Fig. 2, there is a high and narrow peak between the minimum and stop-point, *viz.* between

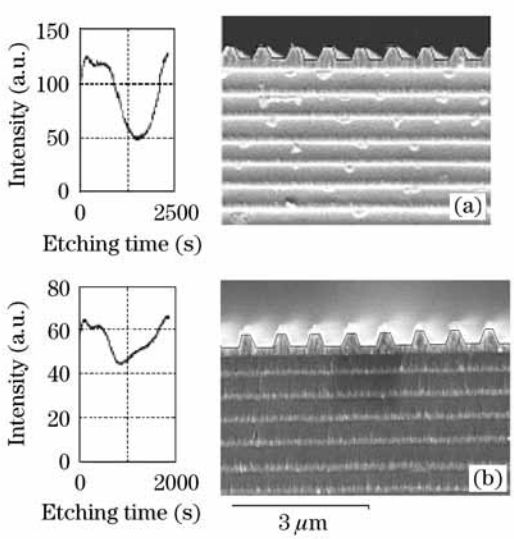

Fig. 3. Monitoring curves and SEM pictures of two resulted gratings. (a) The grating etched for 38 minutes. Efficiency is 92.4% at −1st-order Littrow mount. Efficiency of the reflective order is less than 2%. Original efficiency was 40%. The dark line segments outline the edges of the cross section of the grating. (b) The grating etched for 31 minutes.

points c and d, but this peak does not appear on the experimental curves. The main reason might be that the duty cycles changed during etching. In our experiments, the etched profiles were trapezoidal, and their duty cycles changed from 0.3 to the range of $0.4 - 0.5$. Also, there might be some sputtered material on the grooves and ridges, which could lower the efficiency, as we observed from some SEM pictures of test gratings whose etching was stopped before the optimal end-point. Our finished gratings are not covered by sputtered material. Stopping at the optimal end-point gives us the by-benefit of not needing to clean residual photoresist that is hardened after etching. Another thing that should be pointed out is that the positions and values of the minimum points are different, not only between the simulation (point c) and the real monitoring curves, but also among experiments from run to run. This is mainly caused by the difference between the real and assumed etching rates and the simplification of the evolution model. Tests show that at our ion-beam condition (450-eV ion energy, 89^{+1}_{-9}-mA ion beam current), the etching ratio of photoresist to hafnia ranges from 3 to 6. Experiments also show that the time required to reach the etch stop-point varies with each etching and it could fluctuate by up to 20%. Therefore, it is neither precise nor efficient to control the etching process by time. Owing to the *in-situ* monitoring and end-point detection technique, we do not need to pay much attention to the etching rates of the photoresist and hafnia, and we can obtain acceptable estimates of the etched depth and erosion of the photoresist mask, and thus reduce cost by avoiding excessive measurement of the etching rates of photoresist and hafnia, as well as the improvement in process control.

In summary, we have discussed a practical *in-situ* monitoring and end-point detection method for aiding the fabrication of high efficiency submicrometer period gratings. An empirical profile evolution model is adopted to calculate the −1st-order retro-diffraction efficiency based on the Fourier modal method. The simulation results exhibit the same qualitative features as the *in-situ* monitoring curves. Profiles of the gratings with etching terminated at the estimated optimal point match the design specification quite well, which shows that the proposed *in-situ* end-point detection technique is effective in reproducibly fabricating high efficiency gratings. We have successfully used this technique to fabricate multilayer dielectric gratings with efficiencies of more than 92%.

This research is supported by the National 863 Program of China. H. Lin's e-mail address is linh02@mails.tsinghua.edu.cn.

References

1. B. W. shore, M. D. Perry, J. A. Britten, R. D. Boyd, M. D. Feit, H. T. Nguyen, R. Chow, G. E. Loomis, and L. F. Li, J. Opt. Soc. Am. A **14,** 1124 (1997).
2. K. Hehl, J. Bischoff, U. Mohaupt, M. Palme, B. Schnabel, L. Wenke, R. Bodefeld, W. Theobald, E. Welsch, R. Sauerbrey, and H. Heyer, Appl. Opt. **38,** 6257 (1999).
3. S. Bosch-Charpenay, J. Z. Xu, J. Haigis, P. A. Rosenthal, P. R. Solomon, and J. M. Bustillo, J. Microelectromech. Syst. **11,** 111 (2002).
4. M. M. Bourke, K. P. Hilton, M. A. Crouch, M. J. Kane, N. Borsing, and T. Russell, in *IEEE Workshop on High Performance Electron Devices for Microwave and Optoelectronic Applications* 14 (1995).
5. C. P. Chao, S. Y. Hu, P. Floyd, K-K. Law, S. W. Corzine, J. L. Merz, A. C. Gossard, and L. A. Coldren, IEEE Photon. Technol. Lett. **3,** 585 (1991).
6. A. S. Svakhin, V. A. Sychugov, and A. E. Tikhomirov, Quantum Electron. **24,** 233 (1994).
7. J. S. Zhao, L. F. Li, and Z. H. Wu, Acta Opt. Sin. (in Chinese) **24,** 851 (2004).
8. J. S. Zhao, L. F. Li, Z. H. Wu, Acta Opt. Sin. (in Chinese) **24,** 1285 (2004).